J Geophys (1985) 56:201–210

Journal of Geophysics

Stochastic ion acceleration by coherent electrostatic waves

H. Varvoglis* and K. Papadopoulos

Astronomy Program, University of Maryland

Abstract. The limits of test ion acceleration by electrostatic, coherent, low frequency waves, are examined using the Poincaré surface of section method. The analysis indicates that Hydrogen cyclotron waves preferentially accelerate O^+, while lower hybrid waves favor H^+. This process can be described by a diffusion equation within some phase space boundaries, even for infinite autocorrelation times. Consequences of the results to auroral acceleration are presented.

Key words: Preferential ion acceleration – Auroral Physics – Ion conics formation

Introduction

Particle acceleration in the presence of low frequency electrostatic waves is of paramount importance in the understanding of the spectra of energetic particles in space. A large amount of work has been reported on the various mechanisms for particle acceleration by MHD waves or discontinuities such as the Fermi and shock acceleration processes. It was concluded, in general, that MHD acceleration processes are efficient only for particles above a certain rather large energy threshold, thereby requiring a first stage acceleration. This fact and the observation of energetic particles in regions where MHD waves are absent, motivated the work on the limits of particle acceleration in the presence of short wavelength electrostatic waves (i.e. microturbulent acceleration). The traditional approach follows a quasilinear theory, and computes the energy transfer from the waves to the particles on the basis of an equation of the form (Kennel and Engelman, 1966)

$$\frac{\partial}{\partial t} f = \frac{\pi}{2} \frac{e^2}{M^2} \sum_k \sum_l \frac{1}{k^2} |E_k|^2 \cdot \left\{ \frac{\Omega l}{v_\perp} \frac{\partial}{\partial v_\perp} + k_z \frac{\partial}{\partial v_z} \right\} \cdot J_l^2 \left(\frac{k_\perp v_\perp}{\Omega} \right) \delta(\omega - k_z v_z - l\Omega) \left\{ \frac{\Omega l}{v_\perp} \frac{\partial}{\partial v_\perp} + k_z \frac{\partial}{\partial v_z} \right\} f. \tag{1}$$

This equation can be generalized to include resonance broadening (Dum and Dupree, 1970; Davidson, 1972; Palmadesso et al., 1974), by replacing the delta function $\delta(\omega - k_z v_z - l\Omega)$ by a resonance function $R(\omega - k_z v_z - l\Omega)$. The use of Eq. (1) is subject to the constraints of broadband spectra and small amplitudes, in the sense that $\tau_{AC} \ll \tau_B$, where τ_{AC} is the autocorrelation time of the spectrum and τ_B the bounce time of the resonant particles in the wave. In using quasi-linear theory to describe particle acceleration, for the case where $\omega > \Omega$, we can distinguish two cases. For particles that satisfy the resonance condition $\omega - k_z v_z - l\Omega_j = 0$, we have the usual resonance at the appropriate harmonic number l. The other possibility is to use the unmagnetized theory which requires that

$$\omega = \underline{k} \cdot \underline{v} \tag{2}$$

be satisfied.

Since (Davison 1972) $\tau_B = \left(\frac{eE}{kM} \right)^{-1/2}$, the autocorrelation time restriction implies that

$$E \ll \frac{Mk}{e} \frac{1}{\tau_{AC}^2} \tag{3}$$

where M is the ion mass. Therefore Eq. (1) cannot be applied for particle energization by coherent waves (i.e. $\tau_{AC} \to \infty$). For the ion cyclotron wave observations the autocorrelation time $\tau_{AC} \gg \frac{1}{\Omega_i}$. E.g. for the case discussed by Kintner et al. (1979) where $\tau_{AC} > 10 f_{H^+} \simeq 60\, \Omega_H^{-1}$, and by taking $kR_H \approx 1$ where R_H is the Hydrogen gyroradius, we find $E \ll 10^{-3} \frac{\text{mV}}{\text{m}}$ resulting in exceedingly small wave amplitudes, which will be completely inefficient for acceleration. Therefore neither the magnetized theory nor the unmagnetized theory can be used to describe particle energization by coherent waves.

The observation of perpendicularly accelerated ions in the presence of coherent Hydrogen cyclotron waves (HCW) in the auroral zones (Kintner et al., 1978, 1979; Lysak et al., 1980) is a typical case where a diffusion formalism should not be applied because $\tau_{AC} \gg \tau_B$. An additional problem in attempting to attribute the auroral ion energization to the observed HCW is the presence of energetic O^+ with conic distributions. Since HCW have frequencies $\omega > \Omega_H$, it is not easy to satisfy

* *Permanent address:* Astronomy Department University of Thessaloniki, Greece

Offprint requests to: H. Varvoglis

the resonance condition for any appreciable number of particles of the heavier species, such as O^+. The limitations on the resonant heating of species with $\omega - \Omega_j \gg k_z v_z$ forced Fisk (1978), and Ashour-Abdalla et al. (1981) to postulate, in addition to Hydrogen, excitation of $^4He^+$ and O^+ cyclotron waves respectively.

The limitations and restrictions of the resonant acceleration motivated the work of Papadopoulos et al. (1980), who demonstrated that, in the presence of electrostatic Hydrogen cyclotron waves exceeding a certain amplitude threshold, the maximum non-resonant energization for a subset of particles with a large harmonic number l (i.e. $|\omega - l\Omega_j| \gg k_z v_z$) exceeds by orders of magnitude the resonant one. An additional feature of the mechanism is that stochastic behavior occurs even for infinite autocorrelation time (i.e. monochromatic waves).

The work of Papadopoulos et al. (1980) was based on the intrinsic stochasticity properties of conservative Hamiltonian systems (Chirikov, 1979; Smith and Kaufmann, 1978; Karney, 1979) and was successful in accounting for the preferential perpendicular acceleration of O^+ in the auroral regions. An important corollary was the demonstration that the maximum stochastic acceleration due to Hydrogen cyclotron waves (HCW) scales as $M^{5/2} q^{-3/2}$ with the mass (M) and the charge (q) of the accelerated ions. This paper presents a more detailed account of the process than the space limited short letter of Papadopoulos et al. (1980) and extends the work to include mass ratios $\frac{M}{m_H} < 3$ (where m_H is the Hydrogen mass). A generalized diffusion theory (Karney, 1979), not subject to small amplitude, broad bandwidth constraints [i.e. Eq. (2)], is then applied to examine the observable consequences of the combined action of lower hybrid waves (LHW) and HCW on the auroral particles. A word of caution to the reader is that the emphasis in this paper is on exploring the fundamental physics of the stochastic process under consideration by applying the unified diffusion theory (which is irrespective of the value of the autocorrelation time), rather than trying to do detailed modelling. For this reason we have confined ourselves to the completely non-resonant case by examining waves with $k_z = 0$. This is a good approximation for both the LHW and the HCW, which have $\frac{k_z}{k} \ll 1$.

Finite k_z does not affect the non-resonant processes discussed here to a great extent, but could play an important role in the resonant acceleration or heating of ions (i.e. small harmonic number l) (Abe et al., 1980; Singh et al., 1981; Varvoglis and Papadopoulos, 1984). We will comment on this below in section Non-resonant ion acceleration by electrostatic HCW of this paper.

Basic Problem Formulation

Consider a monochromatic low frequency electrostatic wave

$$\underline{E}(x,t) = \hat{e}_x E_0 \cos(k_\perp x - \omega t) \quad (4)$$

with ω above the Hydrogen cyclotron frequency Ω_H, propagating perpendicular to the ambient magnetic field $\underline{B} = B_0 \hat{e}_z$. Using $cgs-esu$ units the phase space motion of an ion with mass M and charge q, treated as a test particle, is given by the Hamiltonian

$$H = \frac{1}{2M}[P_x^2 + (P_y - qA_y)^2 + P_z^2] - \frac{qE_0}{k_\perp}\sin(k_\perp x - \omega t) \quad (5)$$

where $\underline{A} = A_y \hat{e}_y$ is the vector potential of the ambient magnetic field $\underline{B} = B_0 \hat{e}_z$. We observe that y and z are cyclic coordinates of Eq. (5), so that P_y and P_z are integrals of motion. Therefore, without loss of generality, we may take $P_y = P_z = 0$. Using then the fact that $A_y = x B_0$, Eq. (5) can be written in dimensionless (barred) variables

$$\bar{H} = \tfrac{1}{2}\bar{P}_x^2 + \tfrac{1}{2}\bar{x}^2 - \alpha \sin(\bar{x} - v t) = \bar{h}. \quad (6)$$

In Eq. (6) we have normalized time to Ω_i^{-1} and length to $k_\perp^{-1}$. In these units $\bar{P}_x = \bar{v}_x$, $\bar{x} = \bar{v}_y$, $v = \frac{\omega}{\Omega_i}$ and the wave amplitude is given by

$$\alpha = \frac{k_\perp E_0}{\Omega_i B_0}. \quad (7)$$

If we perform the canonical transformation

$$\bar{x} = (2I_1)^{1/2} \sin\theta_1 \qquad \bar{P}_x = (2I_1)^{1/2}\cos\theta_1$$

$$\bar{t} = \frac{\theta_2}{v} \quad \text{and} \quad \bar{h} = -vI_2$$

where $\bar{h}$ is the numerical value of the Hamiltonian function given by Eq. (6), our Hamiltonian will be given in the action (I_1, I_2) and angle (θ_1, θ_2) variables as

$$H = I_1 + vI_2 - \alpha \sin[(2I_1)^{1/2}\sin\theta_1 - \theta_2]. \quad (8a)$$

Using the Bessel function identity Eq. (8a) becomes

$$H = I_1 + vI_2 - \alpha \sum_{l=-\infty}^{\infty} J_l(r)\sin(l\theta_1 - \theta_2) \quad (8b)$$

where $\frac{1}{2}r^2 = I_1$. Notice that r represents the perpendicular momentum of the particle normalized to $M\frac{\Omega_i}{k_\perp}$. It is beyond the purpose of our paper to discuss the enormous amount of work on non-integrable Hamiltonians of the type (8) over the last few years, referring the interested reader to Jorna (1978) and Helleman (1980) for a detailed exposition. We focus here on the theory of non-integrable Hamiltonian systems as applied to wave-particle interactions.

From Eq. (6) we see that for small α the particle motion is that of a reversible slightly perturbed harmonic oscillator, whose trajectory lies close to a constant energy surface. Above some $\alpha = \alpha_{thr}$, a dramatic transition occurs (often called stochastic instability), at which the particle trajectory in at least a region of phase space becomes chaotic. This allows the particles to cross the surfaces of constant energy (i.e. $I_1 = $const.) in phase space and thus be acclerated or decelerated. Our problem is thus reduced into finding the threshold

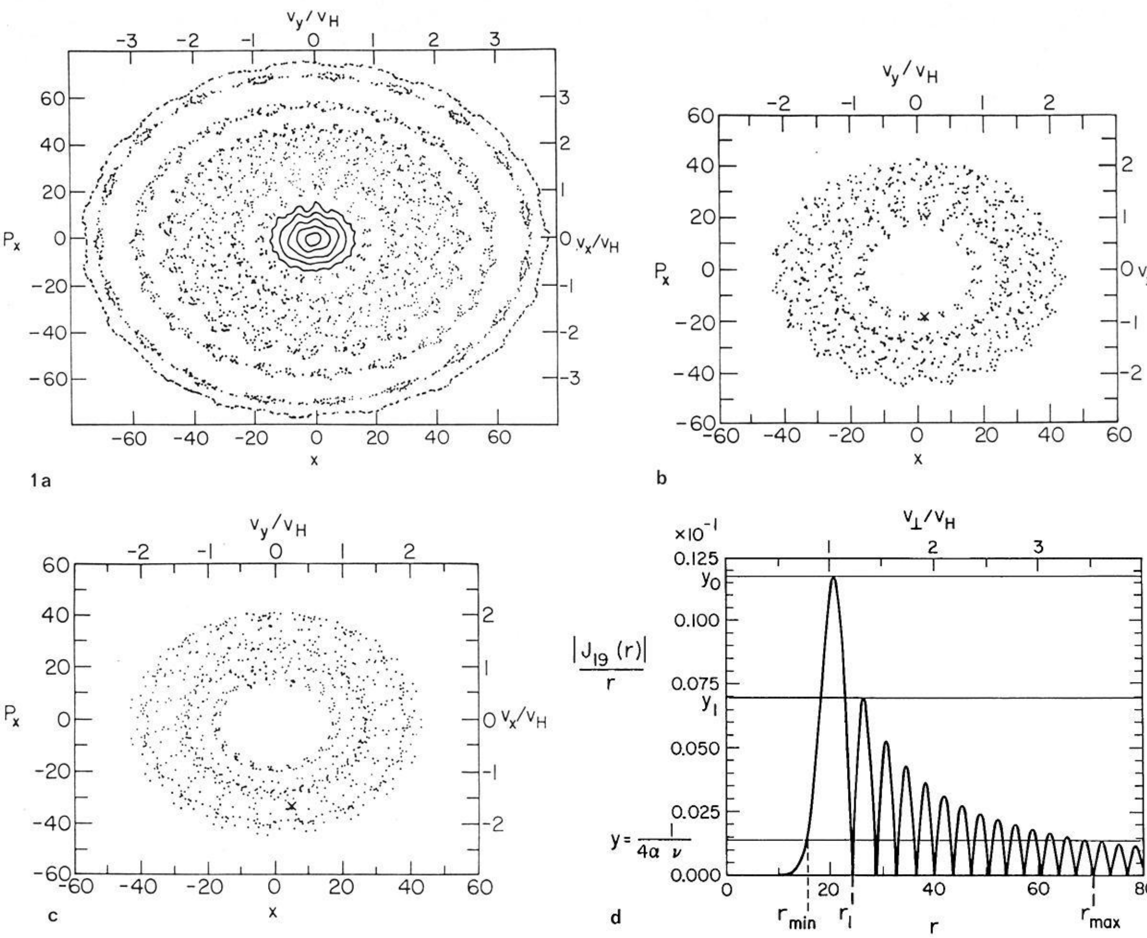

Fig. 1. **a** Surface of section of the system (8) for $\nu = 19.2$, $\alpha = 9$ and for various initial velocities r_0. **b, c** Surface of section of the system (8) for $\nu = 19.2$, $\alpha = 9$ and $r_0 = 18.55$ and 29.15 respectively (r_0 is marked by an x). **d** The function $\left|\frac{J_{19}(r)}{r}\right|$ versus r and graphical calculation of α_{thr}, $r_{\min}$ (approximately) and $r_{\max}$ (upper bound)

value of α, and the upper and lower bounds of the ergodic region in phase space. Before doing this we note an interesting scaling property derived from the definition of α given by Eq. (7). For constant values of B_0 and the wave (i.e. $\bar{E}_0, k_0$), $\alpha \sim \frac{1}{\Omega_i} \sim M_i$, thereby increasing with mass. We expect therefore a mass selectivity, i.e. heavy particles will enter the stochastic region easier. This has been the premise of the Papadopoulos et al. (1980) paper. The value of the threshold α and the bounds of the stochastic region can be found either by a numerical or an approximate analytic method.

The numerical method is based on the concept of surface of section (Birkhoff, 1927; Poincaré, 1957; Berry, 1978). The trajectories describing solutions of the Hamiltonian with $\alpha = 0$ lie on a torus in phase space with major radius $I_2 = \text{const.}$ and minor $I_1 = \text{const.}$ called invariant torus. The angles θ_1 and θ_2 describe the system location on the surface of the invariant torus. A good visualization of the type of trajectories followed by the system can be found by looking at the intersection of the invariant tori with a plane $\theta_2 = \text{const.}$ (we usually take $\theta_2 = \pi$). This is called the surface of section plane. For $\alpha = 0$, the intersections of all the trajectories with the surface of section are points (consequents), lying on concentric circles (invariant curves), each curve corresponding to one trajectory. For $\alpha \neq 0$ and beyond a value of α (threshold value) some trajectories are destabilized and the respective consequents can fill up the space between surviving invariant curves, indicating random motion. By numerically examining the surface of section plots we can find the threshold value (Karney, 1978). This picture is shown in Fig. 1a and will be discussed in the next section.

The analytic method, usually called criterion of overlapping resonances (Rosenbluth et al., 1966; Contopoulos, 1967; Chirikov, 1969, 1979) is based on the following concept. For $\alpha \neq 0$ a canonical perturbation theory of the Hamiltonian given in Eq. (8b) results in a series of resonances (Fukuyama et al., 1977; Lichtenberg, 1979). For finite α each of these resonances cause the appearance of families of islands on the surface of section, with a finite width, monotonically increasing with α. When the size of two neighboring islands belonging to different families becomes such that they touch each other (e.g. overlap), the particles can move across the $I_1 = \text{const.}$ lines and be accelerated. If we apply this criterion to Eq. (8b), we find that the "stochastic" transition occurs for

$$\frac{|J_{[\nu]}(r)|}{r} > \frac{1}{4\nu\alpha} \tag{9}$$

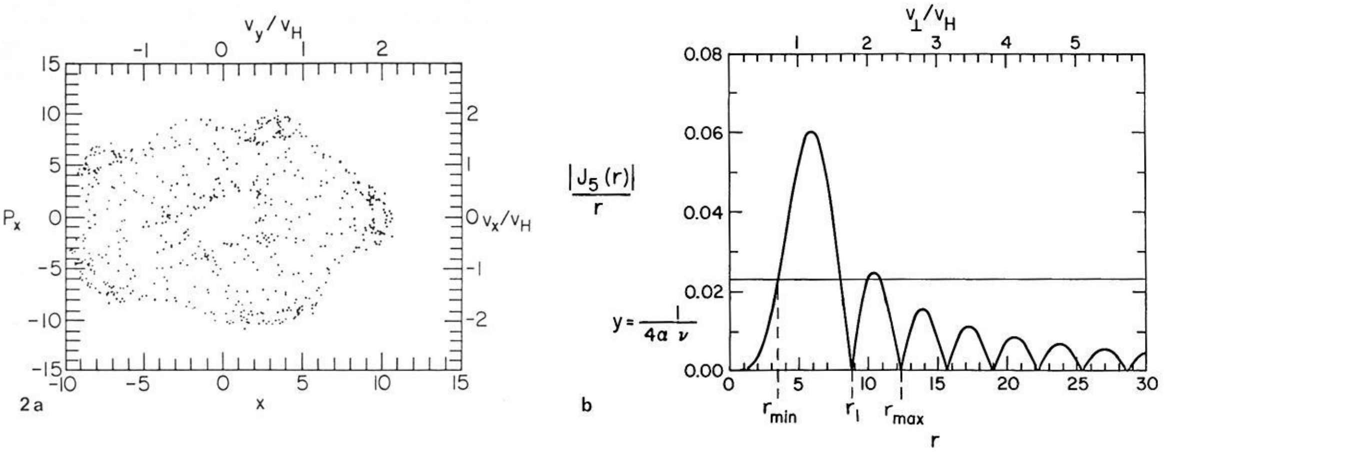

Fig. 2. **a** Surface of section of the system (8) for $\nu = 4.8$, $\alpha = 2.25$ and $r_0 \simeq r_{min}$, **b** The function $\frac{|J_5(r)|}{r}$ versus r and graphical calculation of r_{min} (approximately) and r_{max} (upper bound)

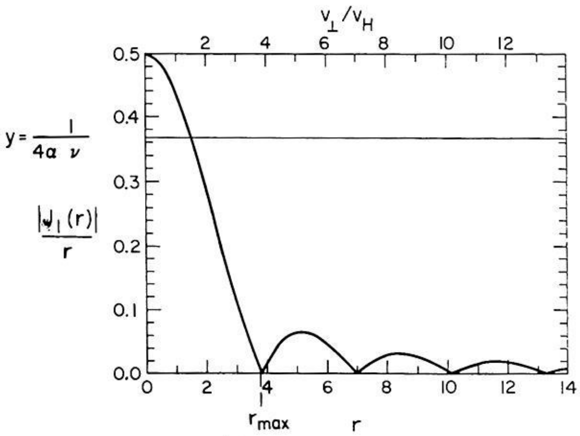

Fig. 3. The function $\frac{|J_1(r)|}{r}$ versus r and graphical calculation of r_{max} (upper bound)

where $[\nu]$ is the integer nearest ν (Fukuyama et al., 1977; Karney, 1978; Lichtenberg, 1979; Abe et al., 1980; Hsu, 1982). Eq. (9) is strictly valid for $r > \nu \geqq 3$ and therefore can give (a) the threshold value of α and (b) the upper bound of the ergodic region in velocity space only in cases when the above condition is satisfied. However a comparison with surface of section plots shows that it gives relatively correct values of α_{thr} and r_{max} when $3 > [\nu] > 1$ (Hsu, 1982) and even acceptable rough estimates of r_{min} when $[\nu] \geqq 1$ (see Figs. 1d, 2b and 3).

Non-Resonant Ion Acceleration by Electrostatic HCW

We proceed next to examine the non-resonant test particle acceleration in the presence of an electrostatic HCW. For the sake of definiteness we use the following parameters:

$$\omega = 1.2\,\Omega_H, \quad k_\perp = (1.5)^{1/2} R_H^{-1} \quad \text{and} \quad \frac{e\phi}{T} \simeq 0.4.$$

These parameters are consistent with the linear theory of the HCW instability (Kadomtsev, 1965) and the observations of the saturated amplitude (Kintner et al., 1978; Böhmer, 1976). There is nothing special about these numbers and can be varied to conform to any other situations under study. We use them here only as basic guidelines for our numerical work. Before exploring the Hamiltonian

$$H = I_1 + \nu I_2 - \alpha \sin(r \sin\theta_1 - \theta_2)$$

using the surface of section method, it is important to stress the strong dependence of our results on the mass ($M = AM_H$) and charge ($q = Qq_H$) of the test ion species under consideration. For a test ion (M, q), and for the parameters mentioned above, the velocity v corresponding to the dimensionless velocity r is given by

$$v(A, Q) = \frac{Q}{A} \frac{r}{(1.5)^{1/2}} v_H \tag{10a}$$

where v_H is the thermal velocity of Hydrogen. The parameters ν and α upon which our Hamiltonian depends are similarly given by

$$\alpha(A, Q) = 1.5 \frac{e\phi}{T} \frac{A}{Q} \tag{10b}$$

and

$$\nu(A, Q) = 1.2 \frac{A}{Q}. \tag{10c}$$

Oxygen ($A = 16, Q = 1$): We examine first the acceleration of O^+. In this case, $\nu = 19.2$ and $\alpha = 9$. Figure 1a shows the surface of section $x - P_x$ for a variety of initial velocities r_0. It is essentially the $I_1\theta_1$ surface in cartesian coordinates. Note that, as was mentioned earlier, $x = v_y$ and $r^2 = x^2 + P_x^2$. For values of $r_0 < 11.5$, corresponding to particle velocities $v < 1/2\,v_H$, the consequents lie on smooth curves indicating that the corresponding trajectories are ordered. For $r_0 = 11.5$ (i.e. $v \approx 1/2\,v_H$), we have an onset of "stochasticity". The connected stochastic region extends to a maximum $r_{max} = 51$ corresponding to $2.6\,v_H$. The ergodic properties of this region are depicted in an illustrative way in Fig. 1b, c. These are surface of section plots for two trajectories: one with initial velocity $r_0 = 18.55$ and the other with $r_0 = 29.15$. Notice how the two trajectories are wondering in the same region of phase space, due to the fact that both are in the connected stochastic region ($11.5<r<51$). If we proceed to increase r_0 past 51, we discover a series of additional small stochastic bands, which are disconnected from the first one and thus we do not expect any particles to reach them, at least on a time scale physically significant to our problem, i.e. $t\simeq 10^3$–$10^4\,\Omega_{O^+}^{-1}$.

We also note that the lower stochasticity threshold $r_0=11.5$ corresponds to 2.3 times the thermal velocity of O^+, and thus only a small fraction (0.2% for a Maxwellian) of O^+ ions can enter the acceleration mechanism. This fraction can be larger if the distribution is non-Maxwellian, e.g. because of resonant acceleration from non-coherent electrostatic noise (Whalen et al., 1978; Klumpar, 1979), but is always small, ensuring our theoretical treatment of O^+ ions as test particles.

We can also find the stochasticity regions for O^+, in the above example, by using the resonance overlap criterion to our problem as given in Eq. (9). The graphical solutions of the inequality is shown in Fig. 1d for the case $[v]=19$. For values of α such that $\frac{1}{4\alpha v}>y_0=\frac{1}{4\alpha_{thr} v}$, the wave amplitude is so small that the particle behaves adiabatically. For values of α such that

$$y_1<\frac{1}{4\alpha v}<y_0$$

only small scale acceleration takes place in the sense that the stochastic region is restricted in the neighborhood of $r\simeq v$ (notice that $r_{min}\simeq\frac{\omega}{k_\perp}=v$, the phase velocity of the wave; this corresponds to the standard quasi-linear result for the unmagnetized case). The maximum velocity that can be achieved is given by r_1, the first zero of the Bessel function (Abe et al., 1980). Finally for

$$\frac{1}{4\alpha v}<y_1$$

large scale non-resonant acceleration is possible. In this case the particle moves towards higher velocities by jumping from one "stochastic cell" to the next across the zeros of the Bessel function J_n (e.g. see MacKay et al., 1984). An upper bound of the maximum velocity r_{max} will be given by the first zero of J_n after the last intersection of the line

$$y=\frac{1}{4\alpha v}, \quad \alpha>\alpha_{thr}$$

with $|J_{[v]}(r)/r|$ (Abe et al., 1980). We emphasize that the so calculated r_{max} is an upper bound, because the last cell satisfying Eq. (9) may not be stochastic over all its width or even it may not be connected to the previous one. For the case of large v and α an analytic expression for inequality (9) can be derived by using the asymptotic expansion for $J_{[v]}(r)$, giving

$$r_{max}=\left[\frac{32\alpha^2 v^2}{\pi}\right]^{1/3}. \tag{11}$$

This is the result used by Papadopoulos et al. (1980) in their discussion of charge to mass ratio scaling in the auroral acceleration of heavy ions.

Helium ($A=4, Q=1$): The He^+ acceleration can be examined along the lines of O^+. In Fig. 2a we give the surface of section for a He^+ trajectory with $r_0\simeq v_{ph}\simeq v_H$. Clearly the diffuse points are wondering inside an annulus whose inner and outer radii give the "barriers" r_{min} and r_{max}. In Fig. 2b we give a graph of the inequality (9) for $n=5$ [as given from Eq. (10c)] and $\alpha=2.25$ $\left[\text{as given from Eq. (10b) for } \frac{e\phi}{T_H}\simeq 0.4\right]$. It can be seen that the efficiency of the acceleration is substantially smaller in this case $\left(\text{the line } y=\frac{1}{4\alpha v} \text{ hardly intersects the second bump of } \frac{|J_5(r)|}{r}\right)$. Numerically the lower threshold r_{min} is found to be $r_{min}=2.4\simeq 0.5\,v_{ph}\simeq 0.5\,v_H$, while the maximum velocity is found to be $r_{max}=10.5\simeq 2.1\,v_H$, corresponding to an energy of $18\,T_H$. Notice how the estimates from the stochasticity criterion (9) compare with the numerically (from the surface of section) determined values of r_{min} and r_{max}, i.e. the inner and outer radii of the stochastic annulus in Fig. 2a.

Hydrogen ($A=1, Q=1$): In this case we expect our criterion (11) to give only a qualitative picture of the behavior of the system, because in deriving (9) terms of the same order as $\frac{J_1(r)}{r}$ where neglected. In Fig. 3 we have plotted the function $\frac{|J_1(r)|}{r}$ versus r as well as the line $y=\frac{1}{4v\alpha}=0.34$. This figure shows that stochastic protons should not have a lower limit in velocity (there are stochastic protons all the way down to $r\simeq 0$), while the maximum velocity should be less than 3.8. These results were confirmed by the numerical method: a surface of section plot shows that the area covered with irregular trajectories is small compared to the cases of Oxygen and Helium, does not have a lower limit in velocity and extends up to $r_{max}\simeq 2.0(\simeq 2v_H)$. It is obvious that protons cannot be accelerated to high perpendicular energies by the HCW even for $\frac{e\phi}{T}\simeq 1$. The amplitude required for the line y to intersect the second bump corresponds to $\frac{e\phi}{T}\gtrsim 2$. We expect therefore that the $\omega-\Omega_i=k_z v_i$ resonant acceleration dominates.

In summarizing the results of this section we note the strong dependence of the acceleration on the mass. This was the main result of Papadopoulos et al. (1980). It is interesting to examine the scaling of the maximum velocity for a wave with $\omega=\bar{v}\Omega_H$, and $k_\perp=\frac{\bar{k}}{R_H}$. Using the asymptotic formula given by Eq. (11), we find for the maximum energy

$$\frac{E_{max}}{T_H}\simeq 5\left(\frac{e\phi}{T_H}\right)^{4/3}(\bar{k}\bar{v}^2)^{2/3}\frac{A^{5/3}}{Q^{2/3}}. \tag{12}$$

In using this formula one should be careful, to be consistent with its validity region for $r>v>3$. Eq. (12) exhibits a strong dependence on A, thereby predicting

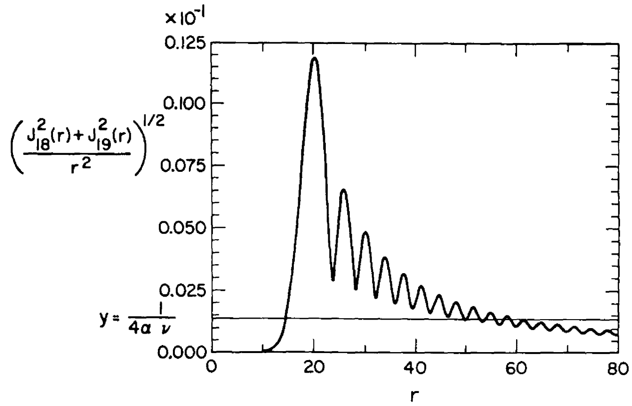

Fig. 4. The function $\frac{[J_{18}^2(r)+J_{19}^2(r)]^{1/2}}{r}$ versus r and graphical calculation of r_{max} for the case of O^+ acceleration, following Lysak et al. (1980)

preferential acceleration of heavy ions. Another interesting feature is the strong dependence on the frequency $\bar{\nu}$ and wavelength $\bar{k}$. For HCW, the value of $\bar{k}$ is of order unity and therefore not an important parameter. However, $\bar{\nu}$ can take values near 2, 3 etc. due to exitation of harmonics. The acceleration due to the first harmonic will dominate only if

$$\frac{\phi_1}{\phi_n} > n$$

where ϕ_n is the wave energy of the n^{th} harmonic. In general the presence of the second harmonic will increase the Helium energy found above, Eq. (12), by a factor

$$\left(\frac{2\phi_2}{\phi_1}\right)^{4/3} = 2.5\left(\frac{\phi_2}{\phi_1}\right)^{4/3}$$

while not affecting the H^+. The H^+ can however enter the stochastic regime by the third harmonic, and reach energies of the order of

$$E_{max} \simeq 40\left(\frac{e\Phi_3}{T_H}\right)^{4/3}.$$

Before closing this section we should comment on the effect of a finite Δk bandwidth in the spectrum, instead of a single wave, and of a finite k_z.

Finite Δk bandwidth

In this case the Hamiltonian of Eq. (5) will be

$$H = \frac{1}{2M}[P_x^2 + (P_y - qA_y)^2 + P_z^2] - q\sum_k \frac{E_k}{k_\perp}\sin(k_\perp x - \omega t). \tag{13}$$

As long as the wave number $\Delta k < k_\perp$, where Δk is the spectrum bandwidth, the analysis can be carried out in a similar fashion as above for each wave-number. The resulting stochasticity criterion will then look like Fig. 4, from which we see that the acceleration limits are not affected.

Finite k_z

The case of a finite k_z has been considered by Abe et al. (1980) and Singh et al. (1981, 1982) who found that finite k_z effects are important for small values of ν (and thus small A/Q) but cannot be neglected even for large ν (and A/Q). As discussed by Karney (1978) and recently by Varvoglis and Papadopoulos (1984) for small $\xi = k_z/k_\perp$ (e.g. $k_z/k_\perp < \frac{1}{3}$) and for $A/Q \gg 1$ the reduced frequency ν in Eq. (9) should be replaced by the Doppler shifted frequency $\nu^* = \nu - \frac{k_z}{k_\perp} p_z$. As a result then Eq. (11) is replaced by the relation

$$r_{max} = \left[\frac{32}{\pi}(\nu^2 - \xi^2 r_{max}^2)\alpha^2\right]^{1/3} \qquad \alpha \geqq \alpha_{thr}$$

which gives estimates for the maximum energization of the ions very close to the numerical results of Singh et al. (1981). Namely for the O^+ energization case considered by Singh et al. (i.e. $\alpha = 18.5$, $\nu = 19.2$) this last equation gives $r_{max} = 84.5$ while Singh et al. find 88.5. This shows that the dominant character of the interaction remains non-resonant, at least for the case of the O^+ ions. However this is not true for H^+ and generally for ions with small A/Q (e.g. $A/Q \lesssim 3$). Note that Eq. (11) and therefore its corrected (for the finite k_z) form cannot be used for the computation of the energization of He^+, since the $A/Q \gg 1$ condition is violated.

Diffusion from Monochromatic Waves

In the previous sections we established the fact that *even a coherent wave* with amplitude above threshold can cause particle diffusion between r_{min} and r_{max} as given before. The basic physical picture is that particles jump from one resonant island to the next. A diffusion coefficient should then be given by $\frac{\langle(\Delta r)^2\rangle}{2\Delta t}$, where Δr is the typical step size and Δt is the corresponding time interval. The change $\langle \Delta r^2\rangle$ in r, between two consecutive "kicks" the particle gets from the wave, is given by $\langle(\Delta r)^2\rangle = \frac{1}{4}, \frac{\alpha^2 n^2}{r^2(r^2 - n^2)^{1/2}}$ (Appendix); this occurs twice at every gyration, that is over time $\Delta t = (2\pi\Omega_i^{-1})/2 = \pi$. The so calculated diffusion coefficient is by a factor of two smaller than the results of Karney (1979) and Antonsen and Ott (1981)

$$D(r) = \frac{1}{2}\frac{\alpha^2 \nu^2}{r^2(r^2 - \nu^2)^{1/2}} \tag{14}$$

that was derived by using standard mapping techniques.

The diffusion equation

$$\frac{\partial f(r,t)}{\partial t} = \frac{1}{r}\frac{\partial}{\partial r} r D(r) \frac{\partial}{\partial r} f(r,t) \tag{15}$$

can be solved exactly if the diffusion coefficient (14) is approximated (for $r \gg \nu$) by

$$D(r) \simeq \frac{1}{2}\frac{\alpha^2 \nu^2}{r^3}.$$

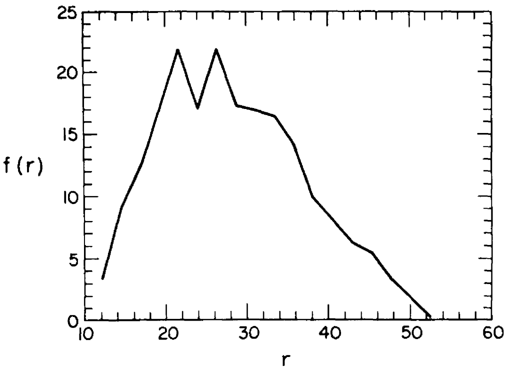

Fig. 5. Distribution function (in arbitrary units) at $t=265$ calculated numerically from a very narrow initial distribution (a "numerical" delta function) at $r_0=14.5$ for $\alpha=9$ and $v=19.2$

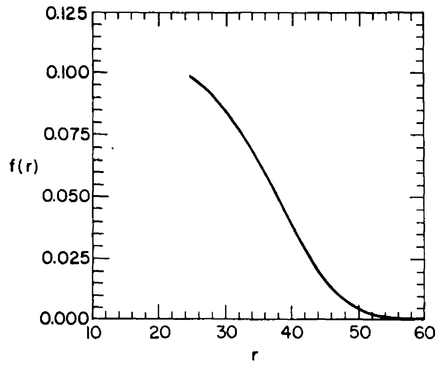

Fig. 6. Solution of the diffusion Eq. (15) (in arbitrary units) at $t=265$ for the same parameter values as Fig. 5

If moreover we take $f(r,0)=f_0(r)=n_0\,\delta(r-r_0)$, then the solution can be written as (Dum, 1978; Wu et al., 1981)

$$f(r,t)=Ct^{-2/5}\exp\left(-\frac{2(r_0^5+r^5)}{25\alpha^2 v^2 t}\right)$$
$$\simeq Ct^{-2/5}\exp\left(-\frac{2r^5}{25\alpha^2 v^2 t}\right) \qquad (16)$$

where we have assumed in the last approximation $r_0 \lesssim v \ll r$. The asymptotic expansions leading to the simple result in Eq. (16) are valid for

$$\frac{4v^5}{25\alpha^2 v^2}=\frac{4v^3}{25\alpha^2}<t\ll\frac{2r_{\max}^5}{25\alpha^2 v^2}\simeq 3.82(\alpha v)^{4/3}.$$

For $\alpha=9$, $v=19.2$ the range of validity is $15<t<3.5\cdot 10^3$, while the typical interaction time in the case of Oxygen acceleration by HCW is of the order of 10^2.

To check how accurately Eq. (16) describes the actual situation, we have performed the following numerical calculations. The trajectories of 100 particles with initial velocities given by a delta function distribution function and identical initial phases $\theta_1=\frac{-\pi}{2}$ where followed in time. Their velocities were recorded at time intervals $\Delta t=2\pi$ and the resulting distribution function was calculated. Figure 5 shows the distribution function calculated in this way for $t=265$ in a case with $\alpha=9$, $v=19.2$, and with a very narrow initial distribution function (a "numerical" delta function) at $r_0=14.5$. To suppress fluctuations due to the small number of particles, Fig. 5, we average $f(r,t)$ over $\Delta t=8\pi$ (i.e. over four recording time intervals).

The distribution function of Fig. 5 should be compared with the solution of the diffusion equation [Eq. (16)], plotted for the same parameter and time values, shown in Fig. 6. Note that this curve starts at $r=24$, because the diffusion coefficient (14) is valid for $r\gg v$ only, and in Fig. 6 we have picked $r>j_{n,1}\simeq n+1.8n^{1/3}$, which for $n=19$ gives $r>24$. We see that the numerical (Fig. 5) and the analytic (Fig. 6) results are in good agreement. The two spikes at $r=22$ and $r=26$ in Fig. 5 are probably due to the presence of an island family at $r\simeq 24$, which has been ignored in the derivation of Eq. (14).

Some Implications of Non-Resonant Acceleration to Auroral Physics

Although the results presented above are very general, with many potential applications to magnetospheric and solar physics, we attempt here to examine some of the implications related to auroral acceleration. In the auroral zones, in addition to HCW, there is substantial wave activity near the lower hybrid frequency. The occurence of lower hybrid waves (LHW) in the auroral zones was discussed by Horita and Watanabe (1969) and later by Papadopoulos and Palmadesso (1975). They usually occur at altitudes lower than the HCW (Mozer et al. 1980). For a strongly magnetized plasma $\left(\text{i.e. } \frac{\Omega_e}{\omega_e}>1\right)$, the lower hybrid frequency Ω_{LH} equals approximately to the Hydrogen plasma frequency ω_H. Since the analysis presented in the previous two sections is valid for waves with frequency $\omega\gtrsim\Omega_i$ it is interesting to examine its implications to the acceleration by LHW.

In the previous section we established the fact that for waves with amplitude above threshold the magnetized and unmagnetized diffusion equation that describes heating or acceleration can be used without the amplitude constraints imposed by the autocorrelation time. In assessing the effectiveness of acceleration of ionospheric ions by LHW we can use either a diffusion approach or a nonlinear test particle analysis. Chang and Coppi (1981) examined the ion energization by LHW using the first approach and assuming a broadband Δk spectrum. For the wave amplitude considered $\left(\text{i.e. } E_{\text{rms}}\simeq 50\frac{\text{mV}}{\text{m}}\right)$, the above assumption is unnecessary since the LHW amplitude is above threshold for non-resonant acceleration of Hydrogen ions by a single wave. We will follow the nonlinear test particle method here, because it allows a direct acceleration efficiency comparison with the HCW and in addition allows us to determine the maximum allowable acceleration (i.e. the velocity at which $D\approx 0$), which is not possible from the diffusion approach. The following standard parameters were taken for the LHW.

$$\omega_{LH}=20\,\Omega_H,\qquad k_\perp R_H=6,\qquad \frac{e\phi}{T_H}\simeq 0.4.$$

Table 1.

Species	E_{min} (ev)		E_{max} (keV)		Relevant time scales in $t\Omega_H$			
	HCW	LHW	HCW	LHW	HCW		LHW	
					Flight	Acceleration	Flight	Acceleration
H^+	0	30	0.05	2.5	2.5×10^3	2.5	3.7×10^4	7×10^3
He^+	10	110	0.25	25	5×10^3	400	7.5×10^4	10^6
O^+	55	450	2.5	250	10×10^3	65×10^3	15×10^4	1.8×10^8

HCW: $\omega=1.2\,\Omega_H$, $k_\perp R_H=(1.5)^{1/2}$, LHW: $\omega=20\,\Omega_H$, $k_\perp R_H=6$, $T_H=10$ ev

These conform with the observed frequency and the expected wave number estimates (Temerin, 1979). No assumption about the bandwidth is necessary since the diffusion process will operate even for coherent waves ($\Delta k=0$). The results are shown in Table 1 where they are compared with the minimum and maximum acceleration limits for HCW. It is obvious from this table that Hydrogen enters easily in the acceleration region for both HCW and LHW, but achieves high energies by non-resonant acceleration only by the LHW. Of course this is in addition to the always present resonant HCW acceleration. On the other extreme reasonable fluxes of He^+ and O^+ can enter the acceleration region for HCW, but only O^+ can be accelerated to substantial energies. Finally acceleration of He^+ and O^+ by LHW is not favored for two reasons. First because of a rather high minimum threshold, and second because of an inefficient acceleration rate. Namely even if some fluxes of He^+ and O^+ enter the stochastic regime, they will drift out of the turbulent region faster than the time scale in which they can gain substantial energy. For example, as it is shown in Table 1, the parallel motion will carry an H^+ ion outside the length $L\simeq 1{,}000$ km of the LHW turbulent region in a time $t_{flight}\simeq 3.7\times10^4\,\Omega_H^{-1}$, an He^+ ion in $7.5\times10^4\,\Omega_H^{-1}$ and an O^+ ion in $15\times10^4\,\Omega_H^{-1}$. This should be compared to the acceleration time scale [the time needed to make the exponent in Eq. (16) unity] which is $t_{scale}\simeq 7\times10^3\,\Omega_H^{-1}$ for H^+, $10^6\,\Omega_H^{-1}$ for He^+ and $1.8\times10^8\,\Omega_H^{-1}$ for O^+ ions respectively.

Before closing we discuss some implications of our results to auroral physics. We limit ourselves to the high energy particles, which cannot be accounted by resonant heating. These are the particles that S 3-3 can measure (i.e. >100 eV). Consider a portion of the auroral field lines around S 3-3 altitudes as shown in Fig. 7, namely a region I with LHW, followed by a region II with HCW at higher altitude. According to our previous results (Table 1) Hydrogen will be selectively accelerated in region I forming high energy conics but will be basically unaffected by HCW in region II, except of course for parallel electric field and mirroring effects which can simply be superimposed in our results. On the other hand O^+ will be unaffected by LHW in region I but accelerated in II. It will be interesting to search in the S 3-3 data for evidence of different regions of conic formation for H^+ and O^+.

We can also speculate with respect to the source of the LHW and HCW. We feel in agreement with Chang and Coppi (1981) and Rowland et al. (1981) that the LHW are excited by the energetic (i.e. keV) electron beams. The LHW waves could create conics in the energetic Hydrogen distribution functions. If these conics move to higher altitudes, they can excite HCW (Mikhailovskii, 1974), which in their turn can form O^+ conics. If the proton conics move downwards an equivalent scenario can be followed. If this is the case the HCW will not be driven by the cold electron current (Kindel and Kennel, 1971) as it is the usual assumption. The above comments are of course very speculative and should be taken as such. We are currently examining this possibility on a detailed basis including non-local effects such as mirror forces and parallel electric fields (Chiu et al., 1981). However, the main point of this section is the fact that the understanding of the non-resonant particle acceleration by low frequency electrostatic turbulence in conjuction with S 3-3 type observations can be very fruitful in resolving basic auroral physics questions, such as the one posed by Kintner et al. (1979): "Did the HCW modes accelerate the ions or the ions excited the waves?" We feel that a closer examination of the S 3-3 data in combination with the physics discussed here can actually help to resolve this ambiguity.

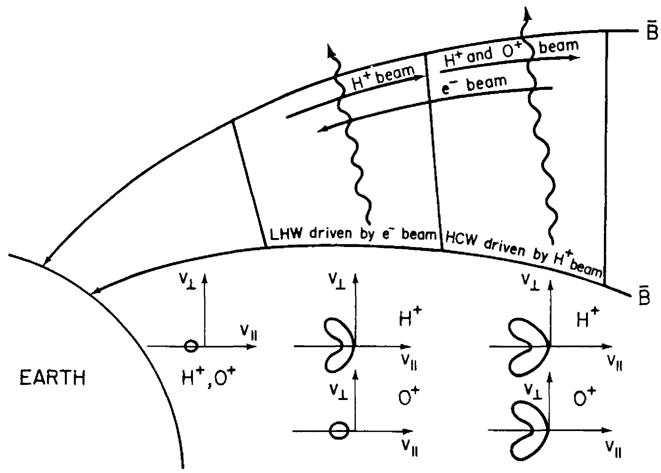

Fig. 7. Proposed scenario for LHW and HCW excitation and H^+, O^+ conics formation in auroral regions

Acknowledgements. This work was supported by NASA NAGW #81 and ONR N00014-79-C0665 grants. Our numerical computations were partially supported by the Computer Science Center of the University of Maryland.

Appendix

Assuming that the chaotic motion of the consequents in velocity space is a Markovian process (Chandrasekhar, 1943) we can compute a diffusion coefficient for the diffusion of ions in phase (and velocity) space in the following way. We find the change Δr in the velocity of an ion that happens in a time interval Δt, and then take the ratio

$$D=\frac{\langle(\Delta r)^2\rangle}{2\Delta t} \tag{A-1}$$

where the average is taken on the surface of section plane $r\theta_1$. As appropriate time interval Δt we take the time needed for an ion to complete one-half gyration around its guiding center, because in one full gyration the particle receives two "kicks" from the wave (one when $p_x \simeq 0$, $x>0$ and one when $p_x \simeq 0$, $x<0$). Accordingly $\Delta t \equiv \frac{2\pi\Omega_i^{-1}}{2} = \pi$ in our system units. The change in velocity in this interval can be calculated from the equations of motion derived from the "resonant" Hamiltonian (Greene, 1980)

$$H_R = I_1 + \nu I_2 - \alpha J_n(r)\sin(n\theta_1 - \theta_2).$$

We find

$$\frac{dI_1}{dt} = r\frac{dr}{dr} = \alpha n J_n(r)\cos(n\theta_1 - \theta_2) \tag{A-2}$$

$$\frac{d\theta_1}{dt} = 1 - \frac{\alpha}{r} J_n'(r)\sin(n\theta_1 - \theta_2) \simeq 1 (\text{since } r \gg \alpha).$$

Then $\frac{dr}{d\theta_1} \simeq \frac{\alpha n J_n(r)}{r}\cos(n\theta_1 - \theta_2)$ and

$$\Delta r \simeq \frac{\alpha n J_n(r)}{r}\cos(n\theta_1 - \theta_2)\Delta\theta_1$$

$$\langle(\Delta r)^2\rangle = \frac{\alpha^2 n^2 J_n^2(r)}{r}\langle\cos^2(n\theta_1 - \theta_2)\rangle\langle(\Delta\theta_1)^2\rangle. \tag{A-3}$$

Because of the already mentioned facts that the particle receives two "kicks" per revolution and $\Delta\theta_1 \simeq \Delta t$, we take $\langle(\Delta\theta_1)^2\rangle = \pi^2$. If moreover we take the average value of (A-3) over a distance $\Delta r = \pi$, we find $\left(\text{assuming that in this distance } \frac{J_n^2(r)}{r^2} \text{ remains practically constant}\right)$

$$D \simeq \frac{\pi}{4}\frac{\alpha^2 n^2}{r^2}\frac{2}{\pi}\frac{1}{(r^2-n^2)^{1/2}}\left\langle\cos^2\left(r - \frac{n\pi}{2} - \frac{\pi}{4}\right)\right\rangle$$
$$= \frac{1}{4}\frac{\alpha^2 n^2}{r^2(r^2-n^2)^{1/2}}.$$

This is by a factor of two smaller than the result obtained by Karney (1979) and by Antonsen and Ott (1981), which we used in solving analytically the diffusion equation (15).

References

Abe, H., Momota, H., Itatani, R.: High-energy tail formation by a monochromatic wave in the magnetized plasma. Phys. Fluids **23**, 2417-2424, 1980

Antonsen, T.M., Jr., Ott, E.: Diffusion coefficient for ions in the presence of a coherent lower hybrid wave. Phys. Fluids **24**, 1635-1640, 1981

Ashour-Abdalla, M., Okuda, H., Cheng, C.Z.: Acceleration of heavy ions in auroral fields lines. Geophys. Res. Lett. **8**, 795-798, 1981

Barbanis, B.: On the Isolating Character of the "Third" integral in a resonance case. Astron. J. **71**, 415-424, 1966

Berry, M.V.: Regular and irregular motion. In: Topics in nonlinear dynamics, S. Jorna, ed. pp. 16-120. New York: American Institute of Physics, 1978

Birkhoff, G.D.: Dynamical systems. New York: American Mathematical Society Colloquium Publications 1927, pp. 143, 152

Böhmer, H.: Excitation of ion cyclotron harmonic waves with an ion beam of high perpendicular energy. Phys. Fluids **19**, 1371-1374, 1976

Chandrasekhar, S., Stochastic Problems in Physics and Astronomy, Rev. Mod. Physics **15**, 1-89, 1943

Chang, T., Coppi, B.: Lower hybrid acceleration and ion evolution in the suprauroral region. Geophys. Res. Lett. **8**, 1253-1256, 1981

Chirikov, B.V.: Research concerning the Theory of Nonlinear Resonance and Stochasticity, Preprint 267 (Institute of Nuclear Physics, Novosibirsk, 1969 (Engl. Transl. CERN Transl. 71-40, 1971)

Chirikov, B.V.: A universal instability of many-dimensional oscillator systems. Phys. Rep. **52**, 264-379, 1979

Chiu, Y.T., Newman, A.L., Cornwall, J.M.: On the structures and mapping of auroral electrostatic potentials. J. Geophys. Res. **86**, 10029-10037, 1981

Contopoulos, G.: Resonance phenomena and the non-applicability of the "third" integral, Bull. Astron. 3e ser. 2, Fasc. 1, 223-241, 1967

Davidson, R.C.: Methods in nonlinear plasma theory. New York: Academic Press, 1972

Dum, C.T., Dupree, T.D.: Nonlinear stabilization of high frequency instabilities in a magnetic field. Phys. Fluid **13**, 2064-2081, 1970

Dum, C.T.: Anomalous heating by ion sound turbulence. Phys. Fluids **21**, 945-955, 1978

Fisk, L.A.: ^{3}He-rich flares, a possible explanation. Astrophys. J. **224**, 1049-1055, 1978

Ford, J.: A picture book in stochasticity. In: Topics in nonlinear dynamics. S. Jorna: ed. pp. 121-146 New York: American Institute of physics, 1978

Fukuyama, A., Momota, H., Itatani, R., Takizuka, T.: Stochastic acceleration by an electrostatic wave near ion cyclotron harmonics. Phys. Rev. Lett. **38**, 701-704, 1977

Green, J.M.: The calculation of K.A.M. surfaces. In: Proc. Int. Conf. on nonlinear dynamics, R. Helleman ed., Ann. N.Y. Acad. Sci. **357**, 80-89, 1980

Helleman, R.H.G.: Self-generated chaotic behavior in nonlinear mechanics. In: Fundamental Problems in Statistical Mechanics Vol. 5, E.G.D. Cohen ed.: pp. 165-233, New York: North Holland 1980

Horita, R.E., Watanabe, T.: Electrostatic waves in the ionosphere excited around the lower hybrid resonance frequency. Planet. Space. Sci. **17**, 61-74, 1969

Hsu, J.Y.: Frequency mismatch and stochastic heating in the cyclotron frequency range. Phys. Fluids. **25**, 159-163, 1982

Jorna, S. (ed): Topics in non-linear dynamics. New York: American Institute of Physics, 1978

Kadomtsev, B.B.: Plasma Turbulence, p. 73. London: Academic Press, 1965

Karney, C.F.F.: Stochastic ion heating by a lower hybrid wave. Phys. Fluids **21**, 1584-1599, 1978

Karney, C.F.F.: Stochastic ion heating by a lower hybrid wave: II Phys. Fluids **22**, 2188-2209, 1979

Kennel, C.F., Engelman, F.: Velocity space diffusion from plasma turbulence in a magnetic field. Phys. Fluids. **9**, 2377-2388, 1966

Kindel, J.M., Kennel, C.F.: Topside current instabilities. J. Geophys. Res. **76**, 3055-3078, 1971

Kintner, P.M., Kelley, M.C., Sharp, R.D., Ghielmetti, A.G., Temerin, M., Cattell, C., Mizera, P.F., Fennell, J.F.: Simultaneous observations of energetic (keV) upstreaming ions and electrostatic hydrogen cyclotron waves. J. Geophys. Res. **84**, 7201-7212, 1979

Kintner, P.M., Kelley, M.C., Mozer, F.S.: Electrostatic hydrogen cyclotron waves near one earth radius altitude in the polar magnetosphere. Geophys. Res. Letters. **5**, 139–142, 1978

Klumpar, D.M.: Transversely accelerated ions: an ionospheric source of hot magnetospheric ions. J. Geophys. Res. **84**, 4229–4237, 1979

Lichtenberg, A.: Adiabatic and stochastic motion of charged particles in the field of a single wave. In: Stochastic behavior in classical and quantum Hamiltonian systems, G. Caseti and J. Ford, (eds).: pp. 18–34, New York: Springer, 1979

Lysak, R.L., Hudson, M.K., Temerin, M.: Ion heating by strong electrostatic ion cyclotron turbulence. J. Geophys. Res. **85**, 678–686, 1980

Mackay, R.S., Meiss, J.D., Percival, I.C.: Transport in Hamiltonian systems. Physica **13D**, 55–81, 1984

Mikhailovskii, A.B.: Theory of plasma instabilities, New York: Consultants Bureau, 1974

Mozer, F.S., Cattell, C.A., Hudson, M.K., Lysak, R.L., Temerin, M., Torbert, R.B.: Satellite measurements and theories of low altitude auroral particle acceleration. Space Sci. Rev. **27**, 155–213, 1980

Palmadesso, P.J., Coffey, T.P., Ossakov, S.L., Papadopoulos, K.: Topside ionosphere ion heating due to electrostatic ion cyclotron turbulence. Geophys. Res. Lett. **1**, 105–108, 1974

Papadopoulos, K., Gaffey, Jr., J.D., Palmadesso, P.J.: Stochastic acceleration of large m/q ions by hydrogen cyclotron waves in the magnetosphere. Geophys. Res. Lett. **7**, 1014–1016, 1980

Papadopoulos, K., Palmadesso, P.J.: Excitation of lower hybrid waves in a plasma by electron beams. Phys. Fluids **19**, 605–606, 1975

Poincaré, H.: Les méthodes nouvelles de la mécanique céleste, Vol. III, p. 75. New York: Dover, 1957

Rosenbluth, M.N., Sagdeev, R.Z., Taylor, J.B., Zaslavski, G.M.: Destruction of magnetic surfaces by magnetic field irregularities. Nucl. Fusion **6**, 297–300, 1966

Rowland, H.L., Palmadesso, P.J., Papadopoulos, K.: Anomalous resistivity of auroral field lines, Geophys. Res. Lett. **8**, 1257–1260, 1981

Singh, N., Schunk, R.W., Sojka, J.J.: Energization of ionospheric ions by electrostatic hydrogen cyclotron waves. Geophys. Res. Lett. **8**, 1249–1252, 1981

Singh, N., Schunk, R.W., Sojka, J.J.: Cyclotron resonance effects on stochastic acceleration of light ionospheric ions. Geophys. Res. Lett. **9**, 1053–1056, 1982

Smith, G.R., Kaufman, A.N.: Stochastic acceleration by an obliquely propagating wave-an example of overlapping resonances. Phys. Fluids **21**, 2230–2241, 1978

Temerin, M.A.: Doppler shift effects on double-probe-measured electric field power spectra, J. Geophys. Res. **84**, 5929–5934, 1979

Treve, Y.M.: Theory of chaotic motion with application to controlled fusion research. In: Topics in nonlinear dynamics. S. Jorna: ed., pp. 147–220. New York: AIP, 1978

Varvoglis, H., Papadopoulos, K.: Large scale chaotic motion of charged particles in a longitudinal electrostatic wave. J. Phys. A **17**, 311–321, 1984

Whalen, B.A., Bernstein, W., Daly, P.W.: Low altitude acceleration of ionospheric ions. Geophys. Res. Lett. **5**, 55–58, 1978

Wu, C.S., Gaffey, Jr. J.D., Liberman, B.: Statistical acceleration of electrons by lower hybrid turbulence. J. Plasma Phys. **25**, 391–402, 1981

Received November 7, 1984; Revised version January 23, 1985
Accepted January 30, 1985